Chinese Journal of Aeronautics, (2014),27(3): 697–707

Chinese Society of Aeronautics and Astronautics
& Beihang University

Chinese Journal of Aeronautics

cja@buaa.edu.cn
www.sciencedirect.com

Inner wrinkling control in hydrodynamic deep drawing of an irregular surface part using drawbeads

Meng Bao [a], Wan Min [a,*], Wu Xiangdong [a], Yuan Sheng [b], Xu Xudong [b], Liu Jie [c]

[a] *School of Mechanical Engineering and Automation, Beihang University, Beijing 100191, China*
[b] *Department of Manufacturing Engineering, Chengdu Aircraft Industrial Corporation, Chengdu 610092, China*
[c] *Sheet Metal Manufacturing Plant, Chengdu Aircraft Industrial Corporation, Chengdu 610092, China*

Received 20 June 2013; revised 23 September 2013; accepted 9 November 2013
Available online 28 April 2014

KEYWORDS

Aircraft part manufacturing;
Drawbead;
Hydrodynamic deep drawing;
Irregular surface part;
Numerical simulation;
Sheet metal;
Wrinkling

Abstract Inner wrinkling phenomenon is more likely to develop during hydrodynamic deep drawing (HDD) of complicated component-forms due to the higher demand for controlling deformation sequences. Aiming at the problems in control of inner wrinkling for an irregular surface part featured with both concavity and convex, this research proposes an optimal design method of drawbead parameters to change the material flow. According to theoretical analysis of the mechanism of inner wrinkling, optimizing cavity pressure only is unreasonable to form a wrinkle-free deep-drawn part, so semi-circular drawbeads are employed. The effects of layout and height of drawbeads on forming results are discussed, and a process window is established based on evaluation indicators including the anti-wrinkle coefficient and the minimum wall thickness. Experiments are carried out to validate the process window, and the wall thickness and the wrinkle height are measured and compared with numerical findings. The results show that the anti-wrinkle ability of drawbeads weakens with increasing oblique angle and distance from the die center, while the wall thickness increases with increasing oblique angle and distance, and the inner wrinkling can be completely suppressed by drawbeads arranged in zones I and II with optimum penetration.

1. Introduction

Wrinkling as one of the major defects in the forming process of various aeronautical parts is becoming more prevalent due to more and more sophisticated designs of sheet metal workpieces in recent years.[1–3] Wrinkling has become a serious obstacle to forming quality and part functions, and finally results in scrap. In addition, wrinkling can damage or even destroy die tools. In order to improve the productivity and quality of products, wrinkling must be prevented.[4,5]

* Corresponding author. Tel.: +86 10 82338788.
E-mail address: mwan@buaa.edu.cn (M. Wan).

Peer review under responsibility of Editorial Committee of CJA.

Production and hosting by Elsevier

1000-9361 © 2014 Production and hosting by Elsevier Ltd. on behalf of CSAA & BUAA. Open access under CC BY-NC-ND license.
http://dx.doi.org/10.1016/j.cja.2014.04.015

Wrinkling is a kind of buckling phenomenon that is resulted from instability under compressive stress. As Wang et al.[6] indicated, two regions of interest where wrinkling occurs are the flange and the unsupported zone between the punch and the die radius, and the latter is called inner wrinkling. However, inner wrinkling appears far more easily than flange buckling when conical parts are formed because of larger unsupported regions. The HDD process, unlike conventional stamping, involves supporting free-form materials with a bed of pressurized fluid during the forming process, which provides tensile frictional forces to reduce the formation of wrinkles. Therefore, the HDD process is widely applied for the manufacture of conical components. In this respect, Yossifon et al.[7,8] predicted the minimum required fluid pressure to suppress wrinkling at the die lip by the energy method, and got the buckling diagram for cylindrical parts. Hsu and Hsieh[9] discussed the wrinkling in the HDD process of hemispherical cups, and performed the lower bound of cavity pressure without the wrinkling failure by applying the in-plane failure criterion and energy method. Abedrabbo et al.[10] investigated the wrinkling behavior of 6111-T4 aluminum alloys during the HDD process, and indicated that the fluid pressure profile greatly affected the wrinkling behavior and the wrinkling could be prevented by optimizing the pressure profile. Ziaeipoor et al.[11] analyzed the effect of hydrostatic pressure on wrinkling phenomenon in the HDD process of hemispherical cups, and obtained 11% improvement in forming depth with hydrostatic pressure in the deep drawing process. Vollertsen and Lange[12] described the reverse drawing wrinkles as a consequence of prostrating of a sheet into a cavity at the beginning of the forming process, and pointed out that the permissible initial pressure was influenced by the punch edge radius. Wu et al.[13] built the working window of counter-pressure for the HDD process of components with stepped geometries, and concluded that the wrinkles could be restrained by properly regulating the fluid pressure. However, if there are conflict areas with respect to required process windows of cavity pressure between concavity and convex features, optimizing the fluid pressure profile independently is unreliable to form a wrinkle-free component possessing both concavity and convex features. Compared with the deep drawing of components having separate concave or re-entrant features, the forming of parts owning both concavity and convex simultaneously is more difficult due to a higher risk of wrinkling and being more difficult to control. Therefore, the manufacture of components with concavity as well as convex characteristics by the HDD process has not been sufficiently investigated.

In this research, the initiation and growth of wrinkling during HDD of a complex surface part with both concavity and convex features were analyzed according to geometric characteristics, and the mechanism of wrinkling was investigated numerically. Furthermore, finite element (FE) simulations were used to optimize the location of drawbeads and investigate the effects of drawbead parameters on the forming quality and wall thickness distributions. Finally, experiments were conducted on a special HDD equipment to fabricate the wrinkle-free part with optimized parameters, and the experimental results were used to validate the numerical observations.

2. Process analysis

2.1. Characteristic of bottom part

The objective part shown in Fig. 1(a) is characterized by a transitional surface from a rectangle to a circle, which is applied in aircraft manufacturing. The addendum surfaces are constructed to adapt the deep drawing process, whose shape and dimensions are illustrated in Fig. 1(b). It can be observed that the length of the rectangular edge is longer than the diameter of the circle, while the width of the rectangle is shorter than the diameter. Thus, the component is featured with both concavity and convex, which is very difficult or even impossible to form by conventional manufacturing methods. Besides, the round edge is regarded as the bottom to decrease the wrinkling trend due to the greater perimeter.[14]

2.2. Used material

Stainless steel 1Cr18Ni9Ti with a thickness of 1.0 mm was employed, and its mechanical properties were obtained by tensile tests. The stress–strain curves achieved under 0°, 45°, and

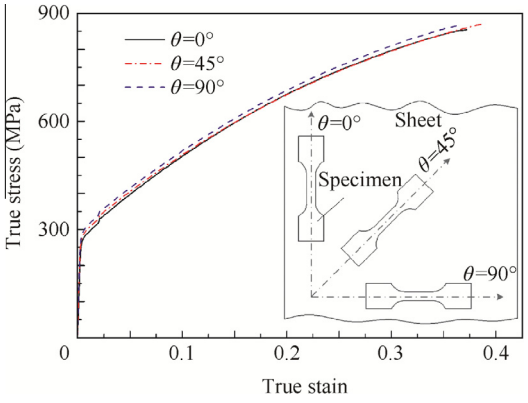

Fig. 2 True stress–strain curves of 1Cr18Ni9Ti.

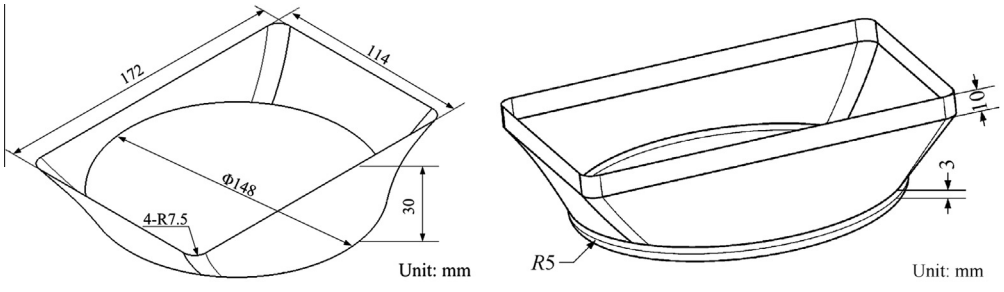

(a) Final part (b) Process supplement

Fig. 1 Irregular surface part and its dimensions.

Table 1 Mechanical properties of 1Cr18Ni9Ti.

Item	Value
Yield strength (MPa)	278
Tensile strength (MPa)	598.5
Hardening coefficient (MPa)	1024
Strain hardening exponent	0.306
Poisson ratio	0.3
Average normal anisotropic coefficient	0.954
Fracture elongation (%)	48.7
Uniform elongation (%)	40.4

90° to the rolling direction θ are shown in Fig. 2, exhibiting a pronounced influence of the rolling direction on the characteristic property values. The basic material parameters are listed in Table 1.

2.3. The guidelines of drawbeads setting

2.3.1. Mechanism of wrinkling

The free-formed area is constantly changing as the increase of punch stroke, and there is a great difference of variation tendency of unsupported areas at different locations. The noncontact regions can be divided into three sections according to the variations of gaps between the punch and the die, as shown in Fig. 3. The free-form regions decrease continuously during the drawing process in the I and II sections, which are characterized by convex features, and the variation degree of zone I is lower than that of zone II. Meanwhile, zone III is characterized by concavity with an increasing interstitial area.

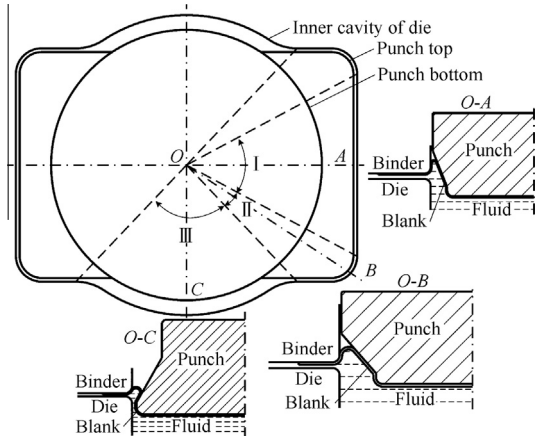

Fig. 3 Variations of unsupported regions at different sections.

The configuration of the punch and the part observed through the *O-D* section is shown in Fig. 4 when the drawing stroke equals to h, in which R_1 is the radius of the round end, R_2 denotes the maximum curvature radius of the punch outline in zone II, p is the fluid pressure, δ_1 and δ_2 are the gaps between the part and the punch outline, respectively. The required materials decrease gradually as the increase of punch stroke because the arc length of blank a_1' is larger than the corresponding length of punch a_1, and the superfluous metals are forced to flow towards both ends of zone III by fluid pressure. Meanwhile, the materials located on the clearance between the punch and the die are imposed to attach to the punch under high pressure in zone II, and a clearance between the blank and the punch will generate on both sides. In other words, the arc length of blank a_2' from tangency point B to the end of zone II is greater than the corresponding length of punch profile a_2, and zonal wrinkles are developed at the junction between zone II and zone III due to the excess materials $a_1' + a_2' - a_1 - a_2$ under the effect of fluid pressure. Once inner wrinkling occurs, the quality and performance of a part are damaged seriously, which results in the scrap of products. The key to restrain inner wrinkling is to prevent materials flowing from zone II to zone III at the initial stage, and control materials flowing form zone III to zone II in the middle-late period.

The forming quality index q in the HDD process can be expressed as:

$$q = F(r_p, r_d, \delta, B, f_b(h), p(h)) \tag{1}$$

where r_p is the punch radius, r_d is the die entrance radius, δ is the gap between the punch and the die, B is the blank shape and dimensions, $f_b(h)$ is the loading path of blank holder force, and $p(h)$ is the path of fluid pressure versus drawing stroke. The effects of r_p, r_d, δ, and B are consistent with conventional deep drawing processes, and can be defined easily according to the geometric features, while $f_b(h)$ can be determined by calculating the counter force on the binder induced by $p(h)$. Therefore, the quality index q can be simplified as:

$$q = F(f_b(p(h)), p(h)) \tag{2}$$

It can be seen that cavity pressure is a critical parameter in the HDD process, which delays the onset of material rupture and also acts as soft drawbeads to control wrinkling in the free-form regions for components with convex features.[15,16]

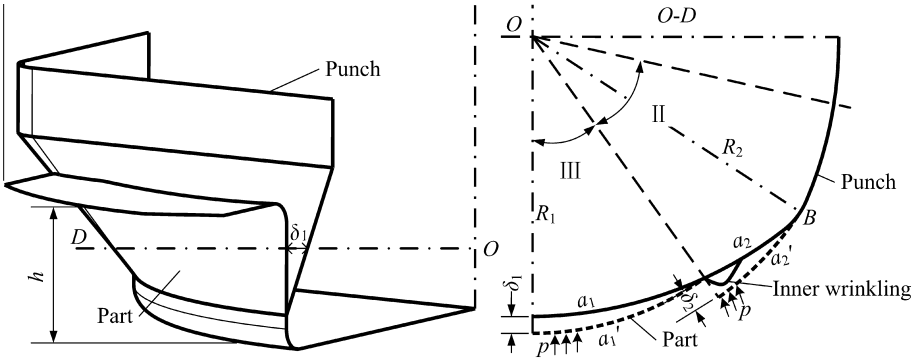

Fig. 4 Generation mechanism of inner wrinkling at junction between zones II and III.

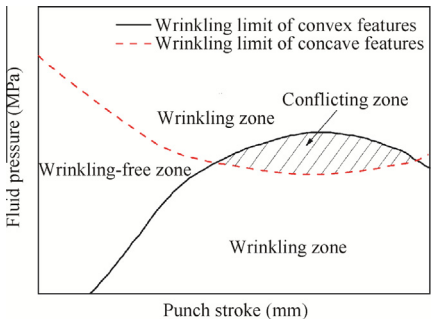

Fig. 5 Schematic of working zone for different features.

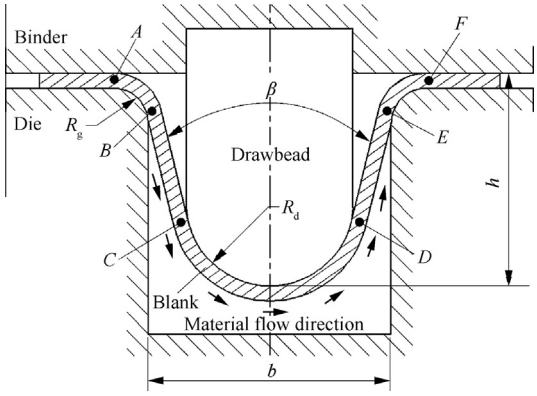

Fig. 6 Development of deformation in a semi-circular drawbead with a square groove.

There is a working zone of counter-pressure for a given part with certain geometric characteristics, and excessive pressure may lead to tearing, while insufficient fluid pressure may result in wrinkling. A reasonable loading path of cavity pressure versus punch stroke within the working zone will ensure producing a deep-drawn part free of rupture or wrinkling. However, finding an appropriate loading path is a critical and difficult step. Since optimizing the loading path of cavity pressure during the HDD process is largely dependent on geometric features, a reasonable loading path cannot be found to adopt different geometrical shapes for irregular components as shown in Fig. 5.

Fig. 5 shows that if the applied pressure is less than the critical wrinkling pressure profile, the fluid pressure will not be high enough to suppress the compressive stress developing on the unsupported regions of parts with convex features, and therefore, causing the material to wrinkle. However, the wrinkling instability will occur when the fluid pressure exceeds the critical wrinkling path because surplus materials are compressed in the circumference of parts with concave characteristics. If there are cross-fields between the two critical wrinkling paths for components with both convex and concave features, the wrinkling phenomenon cannot be prevented by optimizing the loading path of fluid pressure, namely, Eq. (2) cannot be solved with an optimum solution. To prevent inner wrinkling in the HDD process for an irregular part, the method of using drawbeads is put forward, and in this condition, Eq. (2) can be expressed as:

$$q = F'(d, f_b(p(h)), p(h)) \tag{3}$$

where d indicates the parameters of drawbeads.

2.3.2. Principles of drawbeads

The drawbead consists of a bead fixed on the binder surface and a matching groove on the die, as depicted in Fig. 6. The sheet metals undergo bending and unbending deformations on the shoulders of the groove and the bead subsequently as flowing through the drawbead, and the total number of bending and unbending is six, in which the entire restraining force of the drawbead is generated by the work done in the three bending and unbending sequences plus the friction force between the flange and the drawbead.[17,18]

The groove entrance radius R_g, bead radius R_d, penetration height h, groove width b, and bending angle β are the key factors affecting the restraining force of drawbeads among geometric parameters. The restraining force is enhanced with increases of drawbead height, radius, and bending angle.

2.3.3. Evaluation of drawbeads

To study the effect of drawbeads on the forming quality, the evaluation indicator of anti-wrinkle properties is put forward, which is defined as:

$$\eta = \min\left(\frac{t_{ij}}{z_{ij}}\right) \times 100\% \tag{4}$$

where η is the anti-wrinkling coefficient, a lower value of which indicates that the wrinkling is more serious and the anti-wrinkle ability of drawbeads is worse. t_{ij} is the thickness of node j at the cross section through node i, while z_{ij} is the maximum wrinkling height shown in Fig. 7.

The wave height of inner wrinkling can be expressed as:

$$z_{ij} = (b_{ij} - b'_{ij})/2 \quad (i = 0, 1, \ldots, n-1, n; j = 0, 1, \ldots, m-1, m) \tag{5}$$

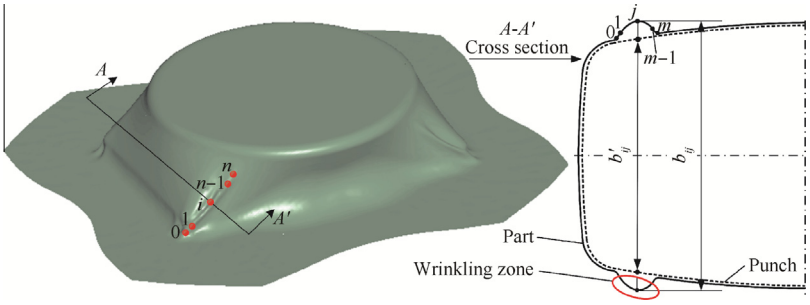

Fig. 7 Schematic diagram of inner wrinkling.

where b_{ij} is the outer edge width of node j at the cross section through node i, b'_{ij} is the width of node corresponding to node j on the punch surface, m and n are the selected nodal numbers.

3. Numerical simulation and experiments

3.1. Numerical simulation

The finite element method (FEM) is thought to be one of the most popular numerical methods in the analysis of sheet metal forming problems, and especially suitable for predicting the deformation process and the failure modes such as wrinkling and local thinning of workpieces with complicated geometries and boundary conditions.[19,20]

In order to reduce the test work regarding to the determination of a process window diagram for drawbead settings, numerical investigations were carried out to observe the details like strain distribution, wrinkling, tearing, and the thinning phenomenon during the HDD process employing the commercial explicit software code eta/Dynaform. The geometries of the drawing tools were modeled, including the punch, the die, the binder, and the blank, as shown in Fig. 8. The die tools were treated as rigid objects without any elastic deformation, while the Belyschko–Tsay, thin shell elements were applied for the square blank, which had a length of 265 mm and a 1.0 mm thickness. The sheets used in experiments clearly exhibited anisotropic characteristics, and it was important to use an appropriate material model that would capture the behavior during the HDD process. Therefore, the three-parameter Baralat's anisotropic material model was used. The semi-circular drawbeads were modeled on the binder surface with a bead radius of 4.0 mm, a groove entrance radius of 5.0 mm, and a groove width of 10.2 mm, and the height could be regulated from 0 mm to 8 mm.

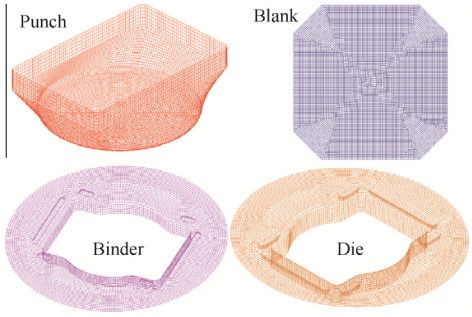

Fig. 8 Numerical model for HDD process.

3.2. Experimental conditions

3.2.1. Tools design

The punch was designed with a separable structure to take off a component from the punch after deep drawing due to the concave features, as presented in Fig. 9(a), and the part could be disengaged from the punch together with the detachable sections of the punch. Adjusting gaskets with a thickness of 1–8 mm were employed to regulate the penetration height of drawbeads, as shown in Fig. 9(b).

3.2.2. Test process

Experiments were carried out on a special double-action HDD press with a capacity of 550 T and fluid pressure of 0–100 MPa, which consisted of a mainframe, a hydraulic control system, and a CNC system. The arrangement of tool dies for the tests was illustrated in Fig. 10.

4. Results and discussion

4.1. Forming result without drawbeads

The HDD process without drawbeads was simulated to analyze the wrinkling phenomenon, and the thickness and strain distributions along the wrinkling zone are shown in Fig. 11. The measurements were performed in the direction of the wrinkling zone starting from the corner of the rectangular end and moving outwardly towards the round edge. Total fifteen points with an equal interval were fixed and the readings were noted at these locations. According to the theory of plastic, the minor stress can be expressed by:

$$\sigma_2 = \lambda\left(\varepsilon_2 + \frac{\overline{R}}{1+\overline{R}}\varepsilon_1\right) \tag{6}$$

where λ is a positive constant called plastic multiplier, ε_1 and ε_2 represent major and minor strains respectively, and $\overline{R}$ is average normal anisotropic coefficient. Compressive stress generates when the minor stress is less than zero, and if the absolute value of the compressive stress is greater than the critical collapsing stress, wrinkling will appear. Therefore,

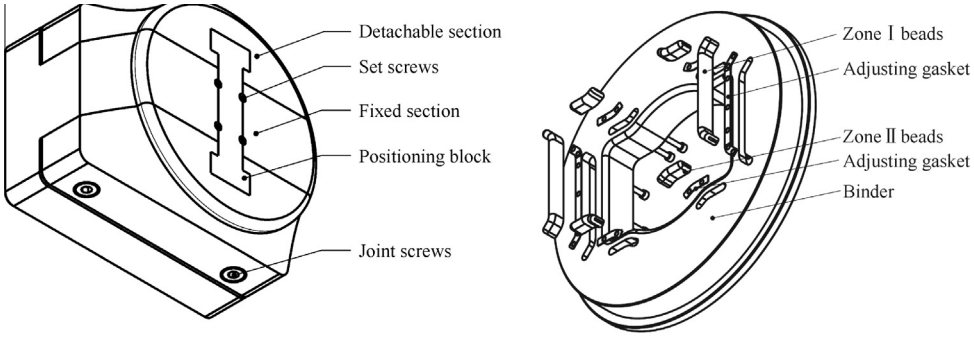

(a) Detachable structure of punch (b) Regulation method of drawbead height

Fig. 9 Structures of punch and the binder.

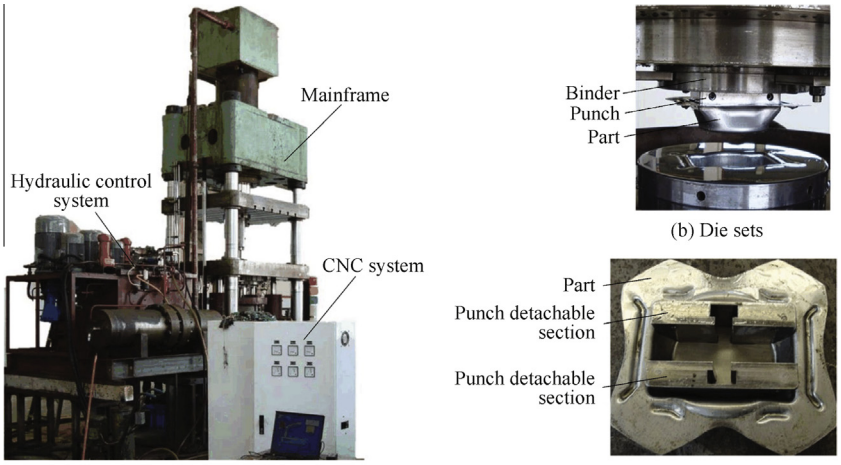

(a) HDD press (b) Die sets (c) Process of taking off a part

Fig. 10 HDD press and die sets.

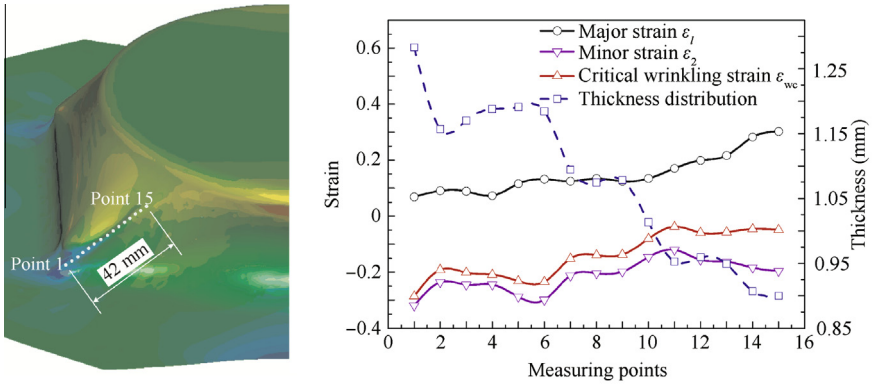

(a) Measuring locations (b) Thickness, major and minor strain distributions

Fig. 11 Thickness, major and minor strains of part without drawbeads.

one of criterions for the wrinkling phenomenon can be defined using strain distributions as:

$$\varepsilon_{wc} = \varepsilon_2 + \frac{\overline{R}}{1+\overline{R}}\varepsilon_1 \tag{7}$$

where ε_{wc} is the critical strain for evaluating wrinkling. It can be observed from Fig. 11(b) that ε_{wc} in the measured zone of the formed part without drawbeads is less than zero, and wrinkling is caused by compressive stress due to inhomogeneous flow of materials at different locations, and at the same time, the thickness distribution is uneven. The fluid pressure plays an active role on the generation of wrinkles along with the alternating change of unsupported regions, and wrinkling is difficult to prevent only by optimizing the profile of pressure versus punch stroke.

4.2. Effect of darwbead parameters on forming quality

Generally, the material in a straight area of a certain drawn component can flow easily into the die, while the material in a corner region flows with difficulty. Therefore, drawbeads should be set on the blank-holder area corresponding to the straight area to make the material in the free-form area flow uniformly. According to the theoretical analysis, drawbeads should be arranged in zones I and II, and the layout of drawbeads is mainly determined by the parameters as presented in Fig. 12. Among them, l_1 and l_2 are the distances from the die center of drawbeads in zones I and II, respectively, while α_1 and α_2 are the oblique angles of drawbeads in zones I and II,

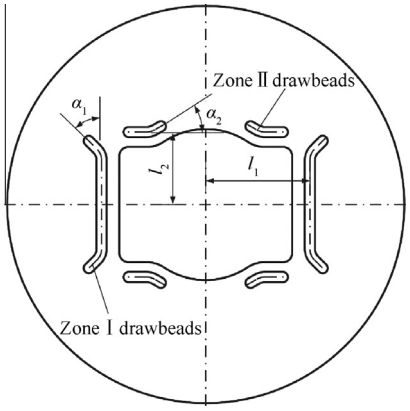

Fig. 12 Parameters of drawbeads.

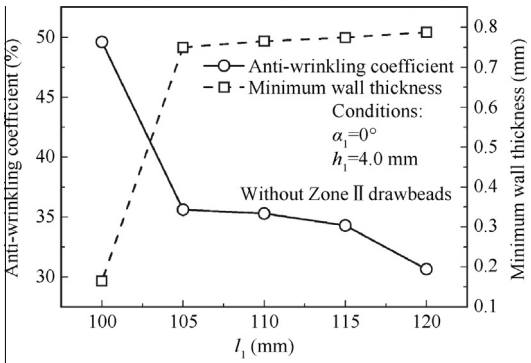

(a) l_1

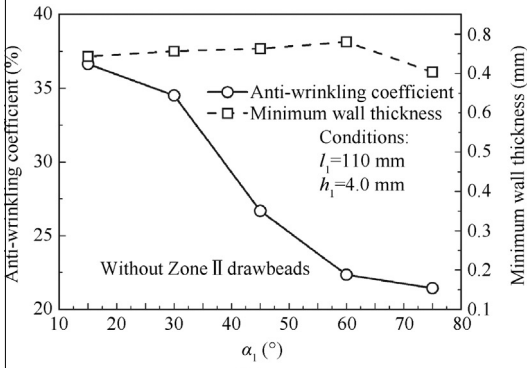

(b) α_1

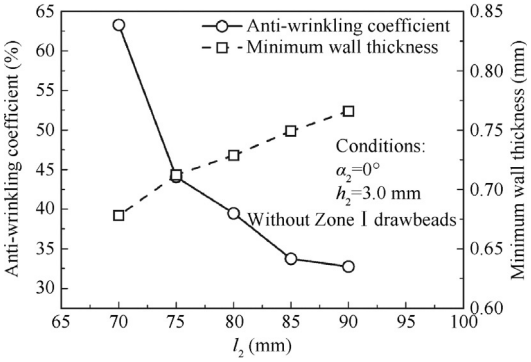

(c) l_2

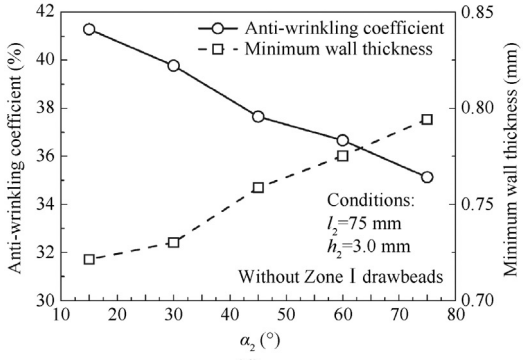

(d) α_2

Fig. 13 Effects of drawbead layout on the forming results.

respectively. Particularly, the oblique angle is set to change the flow direction of materials.

Wrinkling was chiefly induced by non-uniform flow of materials on the irregular surface. To observe the effects of the drawbead layout on the forming results, the anti-wrinkling performances of different arrangements of drawbeads, the wrinkling heights of formed parts, and the minimum wall thickness were measured, as shown in Fig. 13.

It can be observed that the anti-wrinkling property weakened as the increase of the distance from the center of the die, while the minimum wall thickness increased with increasing distance and oblique angle. In addition, it was emphasized that inner wrinkling could not be suppressed completely by employing drawbeads in zone I or zone II individually. Wrinkles appeared in zone II when the drawbeads were set in zone I alone, and similarly, the drawbeads in zone II could not prevent wrinkles in zone I, as depicted in Fig. 14. The comparison of anti-wrinkling properties at different positions is shown in Fig. 15, which indicates that the drawbeads arranged in zone I as well as II can prevent wrinkling efficiently.

Meanwhile, the influence of drawbead penetration on wrinkling was also investigated to obtain the optimum drawbead height, which is illustrated in Fig. 16. Based on the comprehensive consideration of the minimum wall thickness and anti-wrinkling property, the optimal height of zone I drawbeads was 4–5 mm, while the optimized height of drawbeads in zone II was 3 mm.

According to FE simulations, the operating windows for the irregular part were developed to prevent failures like ruptures and wrinkling, as shown in Fig. 17. The process windows provide means for the design and optimization of drawbeads dur-

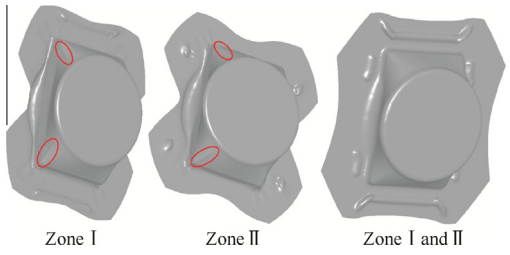

Fig. 14 Effects of drawbead positions on wrinkling.

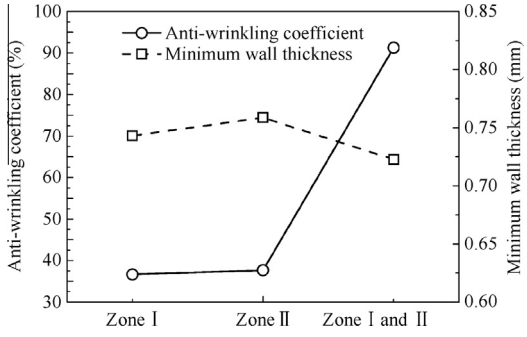

Fig. 15 Comparison of drawbeads at different positions.

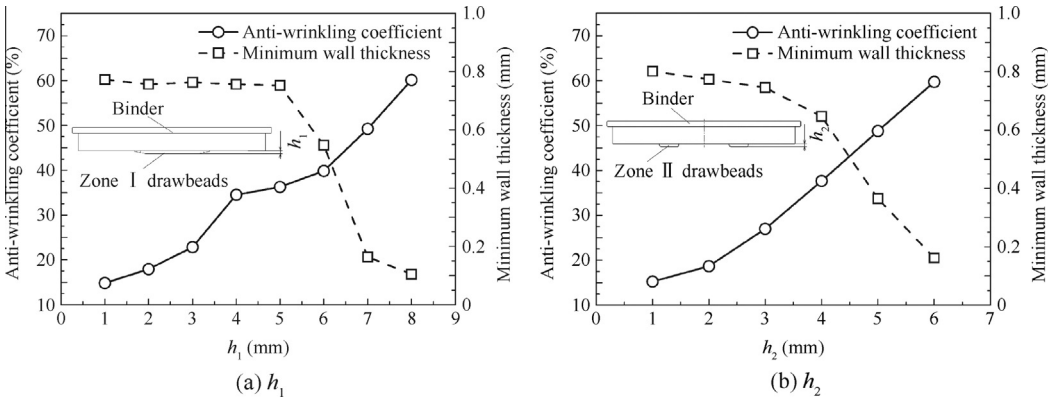

(a) h_1 (b) h_2

Fig. 16 Effects of drawbead penetration on wrinkling.

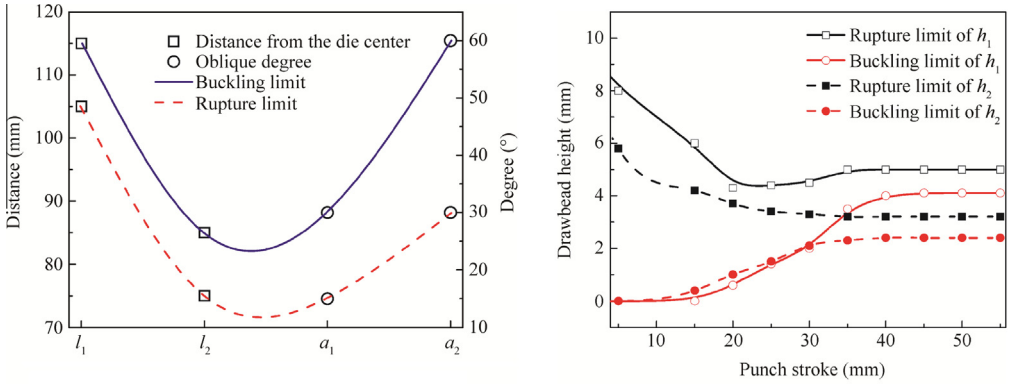

(a) Process window of layout of drawbeads (b) Process window of drawbead height

Fig. 17 Numerical process window diagrams.

ing the HDD process. It can be seen that ruptures are generated with increasing drawbead height and decreasing distance and oblique degree, while the effects of drawbead parameters on the buckling limit are just contrary to the rupture limit.

4.3. Validation of process windows

Experiments were performed with optimized parameters of drawbeads determined by FE simulations including $l_1 = 110$ mm, $\alpha_1 = 15°$, $l_2 = 75$ mm, and $\alpha_2 = 45°$, except the drawbead height h, which could be regulated experimentally. The experimental parts were compared with the predictions obtained from FE simulations. The process windows of drawbead penetration were acquired from experiments by regulating the height of drawbeads, as shown in Fig. 18. It can be seen from Figs. 17(b) and 18 that the optimal height of drawbeads obtained through experiments was in good agreement with the numerical prediction.

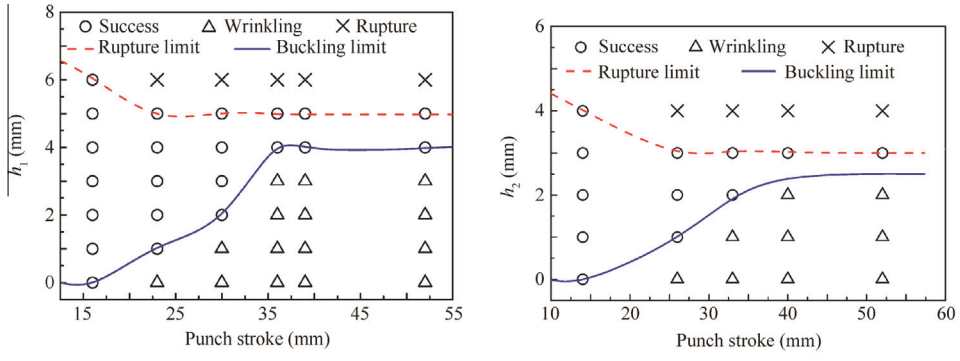

(a) Zone Ⅰ drawbeads (b) Zone Ⅱ drawbeads

Fig. 18 Experimental process windows of drawbead height.

The wrinkling phenomenon shown in Fig. 19 occurred in zone II with $h_2 = 1.0$ mm, and the wrinkling heights measured at 10 locations were obtained for experimental and numerical studies. Generally, the wrinkles tended to have a strip character with a high value in the center and a low value at each end, which was caused by shallow penetration of drawbeads in zone II. It was found that the experimental results were slightly higher than the numerical findings, and the percentage of error in wrinkling height was less than 12%. On the other hand, a larger drawbead height could arouse ruptures in the corresponding regions. The major and minor strains in selected areas of formed parts were measured and mapped to the forming limit diagram (FLD), as indicated in Fig. 20. It can be seen that some measuring points have surpassed the forming limit curve (FLC), indicating that fractures have appeared in the corresponding areas using drawbeads with excessive permeation.

The comparison between FE simulations and experiments with reasonable drawbead penetration was also investigated, and the details of wall thickness measured at 20 locations are given in Fig. 21. The original thickness of 1.0 mm had varied from 0.74 mm to 0.98 mm without considering the flange area, and the maximum reduction of thickness was observed at the bottom of zone III, while the predicted thickness distribution was between 0.72 mm and 1.01 mm, which was in close agreement with experiments.

After the processes of trimming and solution treatment, the final component was fabricated, as presented in Fig. 22. It is also observed that the wrinkling phenomenon of the irregular

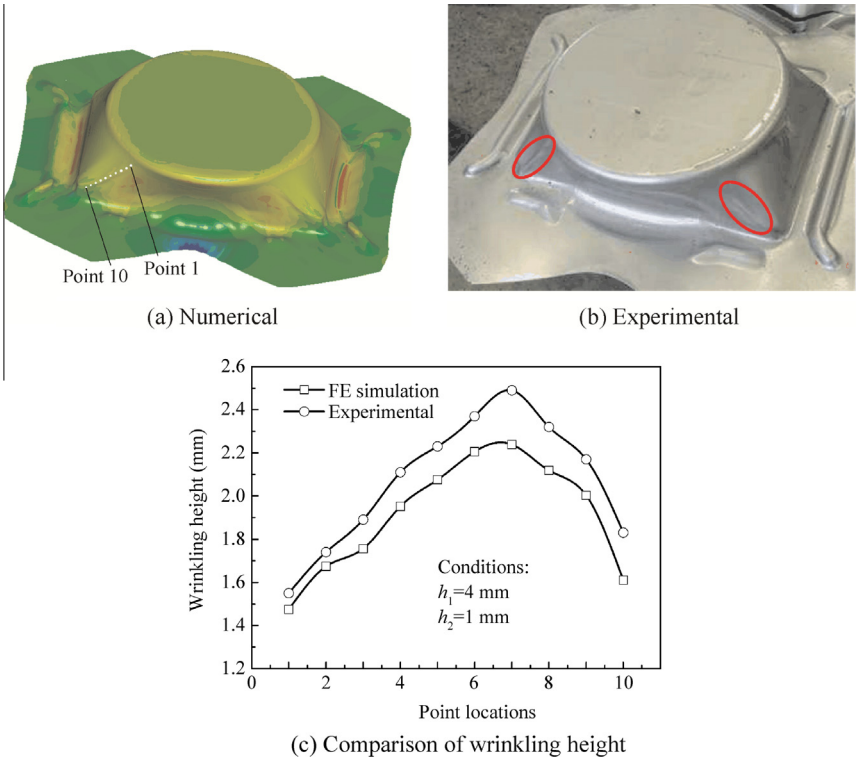

Fig. 19 Wrinkling phenomenon caused by shallow drawbead penetration.

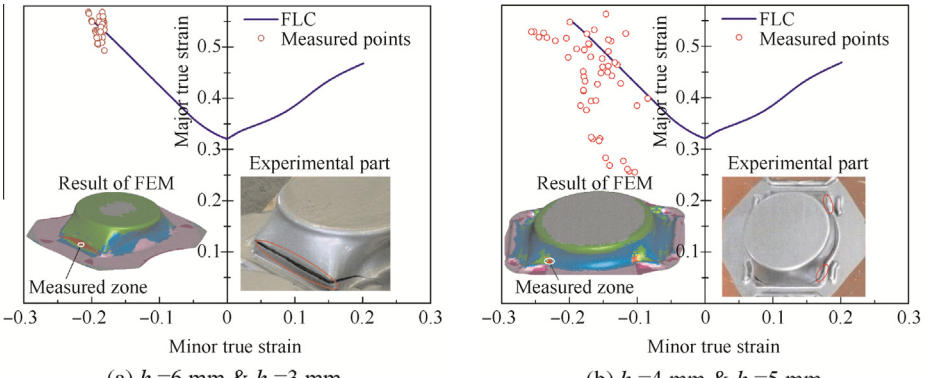

Fig. 20 Ruptures caused by too deep drawbead penetration.

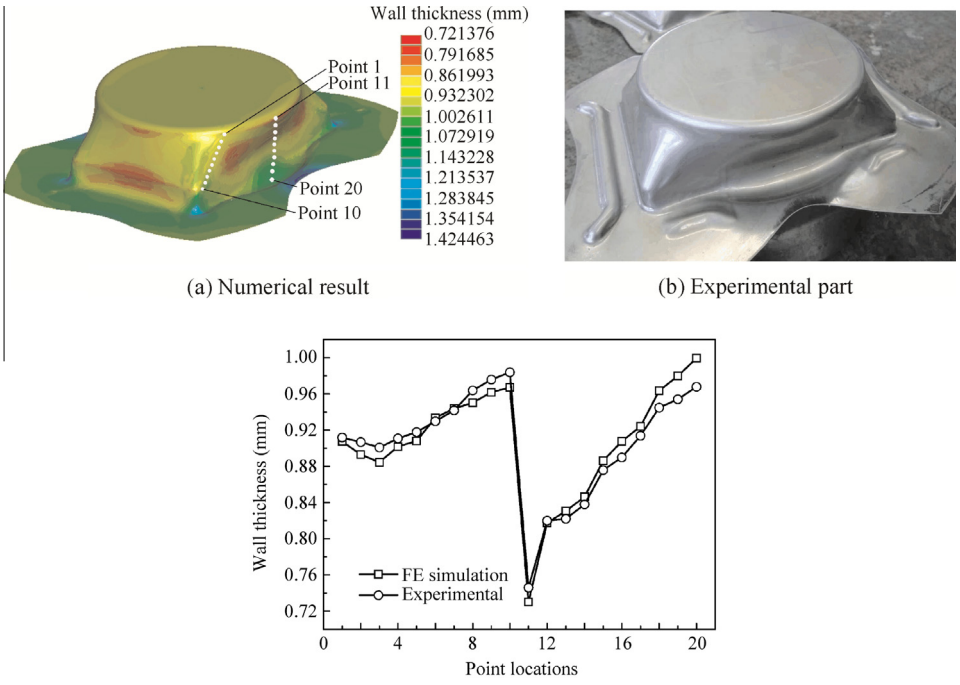

Fig. 21 Formed component with drawbeads of $h_1 = 4.0$ mm and $h_2 = 3.0$ mm.

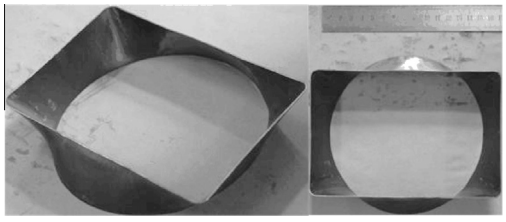

Fig. 22 Final parts.

surface part induced by non-uniform flow of materials can be suppressed completely by employing drawbeads with optimized parameters.

5. Conclusions

(1) Inner wrinkling in the HDD process of an irregular surface part featured with both concavity and convex is mainly aroused by non-uniform flow of materials associated with continuous variations of gaps between the punch and the die. Since the loading path of cavity pressure is largely dependent on geometric features and a reasonable loading path for concave features is contrary to that for convex characteristics, only optimizing pressure profile is impossible to prevent the inner wrinkling.

(2) The anti-wrinkling coefficient η is put forward to evaluate the effect of drawbeads, and η weakens with increasing l_1, α_1, l_2, and α_2, while the minimum wall thickness increases with increases of l_1, α_1, l_2, and α_2.

(3) Inner wrinkling cannot be suppressed completely by using drawbeads in zone I or zone II individually, and the value of η increases from 35% with independent drawbeads to 91% with drawbeads arranged in zone I as well as zone II.

(4) Shallow drawbead penetration cannot prevent the occurrence of inner wrinkling, while large drawbead height results in ruptures. In consideration of the minimum wall thickness and anti-wrinkling property, the optimum height of zone I drawbeads is 4–5 mm, while the appropriate height of drawbeads in zone II is 3 mm.

(5) Experiments were carried out employing the optimized parameters of l_1, α_1, l_2, and α_2, and the effects of drawbead height on the wrinkling height and thickness distributions were compared with numerical findings. It is observed that the numerical results are very close to the experimental observations, and the FE method for parameter optimization of drawbeads is far superior to the costs that would accrue if each parameter is actually built and tested.

Acknowledgements

All the experiments were financed and supported by Chengdu Aircraft Industrial Corporation. Meanwhile, the authors acknowledge Dr. Chu Wang and Zheng Jiang for English polishing and spell checking. They are also very grateful to the editors and the reviewers for their critical and constructive suggestions of the manuscript.

References

1. Narayanasamy R, Narayanan CS. Wrinkling behavior of interstitial free steel sheets when drawn through tapered dies. *Mater Des* 2007;**28**(1):254–9.

2. Shafaat MA, Abbasi M, Ketabchi M. Investigation into wall wrinkling in deep drawing process of conical cups. *J Mater Process Technol* 2011;**211**(11):1783–95.
3. Tian S, Liu YL, Yang H. Effects of geometrical parameters on wrinkling of thin-walled rectangular aluminum alloy wave-guide tubes in rotary-draw bending. *Chin J Aeronaut* 2013;**26**(1):242–8.
4. Abbasi M, Ketabchi M, Labudde T, Parhi U, Bleck W. New attempt to wrinkling behavior analysis of tailor welded blanks during the deep drawing process. *Mater Des* 2012;**40**:40714.
5. Liu JG, Wang ZJ. Prediction of wrinkling and fracturing in viscous pressure forming (VPF) by using the coupled deformation sectional finite element method. *Comput Mater Sci* 2010;**48**(2):381–9.
6. Wang CT, Kinze G, Altan T. Wrinkling criterion for an anisotropic shell with compound curvatures in sheet forming. *Int J Mech Sci* 1994;**36**(10):945–60.
7. Yossifon S, Tirosh J, Kochavi E. On suppression of plastic buckling in hydroforming processes. *Int J Mech Sci* 1984;**26**(6):389–402.
8. Yossifon S, Tirosh J. The maximum drawing ratio in hydroforming processes. *J Manuf Sci Eng* 1990;**112**(1):47–56.
9. Hsu TC, Hsieh SJ. Theoretical and experimental analysis of failure for the hemisphere punch hydroforming processes. *Trans ASME* 1996;**118**(3):434–8.
10. Abedrabbo N, Zampaloni MA, Pourboghrat F. Wrinkling control in aluminum sheet hydroforming. *Int J Mech Sci* 2005;**47**(3):333–58.
11. Ziaeipoor H, Jamshidifard S, Moosavi H, Khademizadeh H. Numerical analysis of wrinkling phenomenon in hydroforming deep drawing with hemispherical punch. In: Fujita H, Sasaki J, editors. *Proceedings of the 9th WSEAS international conference on system science and simulation in engineering; 2010 October 4–6; Iwate, Japan*. Wisconsin: WSEAS; 2010. p. 96–102.
12. Vollertsen F, Lange K. Process layout avoiding reverse drawing wrinkles in hydroforming of sheet metal. *CIRP Ann Manuf Technol* 2002;**51**(1):203–8.
13. Wu J, Balendra R, Qin Y. A study on the forming limits of the hydromechanical deep drawing of components with stepped geometries. *J Mater Process Technol* 2004;**145**(2):242–6.
14. Meng B, Wan M, Wu XD, Yuan S, Xu XD, Li GJ. Research on failure control of hydroforming deep drawing for complex surface part. *Acta Aeronaut Astronaut Sin* 2010;**31**(12):2457–63 [Chinese].
15. Qin Y, Balendra R. Design considerations for hydromechanical deep drawing of sheet components with concave features. *J Mater Process Technol* 2004;**145**(2):163–70.
16. Dao TP, Huang SC. Study on optimization of process parameters for hydromechanical deep drawing of trapezoid cup. *J Eng Technol Educ* 2011;**8**(1):53–71.
17. Samuel M. Influence of drawbead geometry on sheet metal forming. *J Mater Process Technol* 2002;**122**(1):94–103.
18. Sheriff NM, Ismail MM. Numerical design optimization of drawbead position and experimental validation of cup drawing process. *J Mater Process Technol* 2008;**206**(1):83–91.
19. Sharma AK, Rout DK. Finite element analysis of sheet hydromechanical forming of circular cup. *J Mater Process Technol* 2009;**209**(3):1445–53.
20. Yan Y, Wan M, Wang HB, Huang L. Design and optimization of press bend forming path for producing aircraft integral panels with compound curvatures. *Chin J Aeronaut* 2010;**23**(2):274–82.

Meng Bao is a Ph.D. student in the School of Mechanical Engineering and Automation at Beihang University. He received his B.S. degree in aircraft manufacturing engineering from Beihang University in 2008. His main research interests are HDD process and equipment, vacuum thermal deep drawing process and equipment.

Wan Min is a professor and Ph.D. advisor in the School of Mechanical Engineering and Automation at Beihang University. He received his Ph.D. degree from Harbin Institute of Technology in 1995. His area of research includes advanced plastic forming technology and equipment, digital forming technology, sheet metal plastic forming theory and experimental technology.